Synthesis, characterization and crystal structure of cadmium(II) nano coordination compound: A precursor to produce nano-sized cadmium oxide and cadmium iodide

Maryam Ranjbar [a],[*], Mostafa Yousefi [a], Robabeh Nozari [b], Shabnam Sheshmani [b]

[a] *Department of Chemical Technologies, Iranian Research Organization for Science and Technology (IROST), Tehran, Iran*
[b] *Department of Chemistry, College of Basic Sciences, Yadegar-e-Imam Khomeini (RAH) - Shahr-e Rey Branch, Islamic Azad University, Tehran, Iran*

Abstract

In this research, a cadmium(II) nano coordination compound, [Cd(dmph)I$_2$] (1), {dmph= 2,9-dimethyl-1,10-phenanthroline (neocuproine)}, was synthesized by sonochemical method from cadmium(II) acetate, KI and the neocuproine ligand. The nano-structure (1) was characterized by scanning electron microscopy (SEM), X-ray powder diffraction (XRD), elemental analyses and IR spectroscopy. The compound 1 was structurally characterized by single crystal X-ray diffraction and showed that Cd(II) ion is four-coordinated in a distorted tetrahedral configuration with two N atoms from a neocuproine ligand and two terminal iodine atoms. The thermal stability of compound 1 both in its bulk form and nano-size form had been studied by thermal gravimetric (TG) and differential thermal analyses (DTA) for comparsion with each other. Pure phase CdO and CdI$_2$ nanoparticles were prepared by calcination of compound 1 at 700 $^\circ$C under air atmosphere and hydrothermal processing from the same compound at 150 $^\circ$C for 48 h, respectively. The morphology and phase of the prepared samples were further studied using SEM and XRD. The sonochemical method resulted in a significant reduction of reaction time, reaction temperature and particle sizes of the products.

Keywords: Coordination compound; Nano CdO; Nano CdI$_2$; Neocuproine; Sonochemical method.

1. Introduction

Properties of materials strongly depend on both the size and the morphologies of the microscopic particles. Many properties undergo drastic changes when their particle sizes are smaller than a micron in at least one dimension. In these nano-scale materials, or simply nanomaterials the ratio of surface area to volume is vastly increased when compared to compounds with larger grain sizes. Quantum mechanical effects such as the ''quantum size effect'' begin to play a significant role when the same compound is in nano size. These effects play a minor role when going from macro to micro dimensions, but become increasingly significant when their particle size reaches the nanometer range.

[*] .**Corresponding author***:* Associate Professor of Inorganic Chemistry, Research Institute of Chemical Technology, Iran Scientific and Industrial Research Organization *E-mail address: marandjbar@irost.ir*

More importantly electronic properties of solids are altered substantially with such reductions in particle size. Besides, a number of other physical properties such as catalytic activities change when compared to macroscopic systems [1]. Metal coordination compounds have been widely studied as they represent an important interface between synthetic chemistry and materials science. The synthesis of metal coordination compounds with different metal ions and ligands [2,3] have led to a wide range of potential applications such as molecular wires [4], electrical conductors [5], molecular magnets [6] and various applications in host–guest chemistry [7], catalysis [8] and etc. In contrast to nanomaterials made up from inorganic extended solids, research in specific syntheses of nano-structured metal coordination compounds using sonochemical methods seem to be comparatively scarce.

Cd^{2+}, as a d^{10} metal ion, is particularly suited for the construction of supramolecular compounds and networks. The spherical d^{10} configuration is associated with a flexible coordination environment, such that geometries of these complexes can vary from tetrahedral (CN= 4) to dodecahedral (CN= 8) with possibility of severe distortions in the ideal polyhedron. Furthermore, due to the general lability of Cd(II) complexes, the formation of coordination bonds is reversible, which enables metal ions and ligands to rearrange during the process of polymerization to give highly ordered network structures. Consequently, Cd can readily accommodate all kinds of architectures and a selection of topological types of 1D, 2D and 3D polymers [9-12]. Thus, their preparation is challenging owing to their ability to tailor their physical and chemical properties [13]. On the other hand, cadmium oxide ($E_g \sim 2.3$ eV) is an n-type degenerate semiconductor with high electrical conductivity. Due to its large linear refractive index ($n_0 = 2.49$), it is a promising candidate for optoelectronic applications and other applications including solar cells, photo transistors, photodiodes, transparent electrodes and gas sensors [14,15]. Because of these interesting applications, efforts to prepare nanoparticles of CdO using a variety of methods have been reported in the literature [16-18]. Among others, solvothermal synthesis [19] and a microemulsion method [20] have been reported for preparing CdO nanoparticles.

In this paper, we report the sonochemical preparation and crystal structure of a cadmium(II) nano coordination compound, [Cd(dmph)I_2] (1), (dmph= 2,9-dimethyl-1,10-phenanthroline), and its use as a precursor for the preparation of CdO and CdI$_2$ nanoparticles. 2,9-dimethyl-1,10-phenanthroline (dmph) is an attractive bidentate ligand, and numerous complexes have been prepared with it, such as those of mercury, zinc, copper, cobalt and etc. [21-24]. The results reveal that compared with traditional synthetic techniques, such as solvent diffusion technique, hydrothermal and solvothermal methods, the ultrasonic synthesis is a simple, low cost, efficient, and environmentally friendly approach to nano-scale coordination supramolecular compound [25]. Sonochemical methods can lead to homogeneous nucleation and a substantial decrease in crystallization time compared with conventional oven heating when nanomaterials are prepared [26]. Many researchers have investigated the effect of ultrasound on chemical reactions, and most theories imply that the physical or chemical effects of ultrasound originate from acoustic cavitation within collapsing bubbles, which generates extremely localized hot spots having pressures of about 1000 bar, temperatures of roughly 5000 K, and heating and cooling rates of about 10^{10} Ks^{-1}. Between the microbubble and the bulk solution, the interfacial region around the bubble has very large gradients of pressure, temperature, and the rapid motion of molecules leading to the production of excited states, bond breakage, the formation of free radicals, mechanical shocks, and high shear gradients [27]. The use of high-intensity ultrasound to enhance the reactivity of metals as a stoichiometric reagent has become a synthetic technique for many heterogeneous organic and organometallic reactions [28-34].

2. Experimental procedure

2.1. Materials and physical measurements

All reagents and solvents used in this work were commercially available and employed without further

purification. A multiwave ultrasonic generator (Sonicator-4000; Misonix, USA), equipped with a converter/transducer and titanium oscillator (horn), 12.5 mm in diameter, operating at 20 KHz with a maximum power output of 600 W, was used for ultrasonic irradiation. The ultrasonic generator automatically adjusts the power level. Melting points were measured with a Thermo Scientific 9200 apparatus and are uncorrected. Elemental analyses (carbon, hydrogen, and nitrogen) were performed using a Heraeus CHN–O– Rapid analyzer. FT-IR spectra were recorded on a Bruker tensor 27 spectrophotometer in the range 400–3500 cm^{-1} using the KBr disk technique. X-ray powder diffraction (XRD) measurements were performed using a Philips X'pert diffractometer with monochromated Cu-K$_\alpha$ (λ= 1.5418 Å) radiation at room temperature in the 2θ range of 10-90°. The crystallite sizes of selected samples were estimated using the Scherrer formula. The simulated XRD powder pattern based on single crystal data were prepared using Mercury software [35]. Thermogravimetric analysis (TGA) and differential thermal analyses (DTA) of the title compound were performed on a computer-controlled PL-STA 1500 apparatus. Powder sample of 1 was loaded into alumina pans and heated with a gradient rate of 10 $^\circ$C/min from room temperature to 600 $^\circ$C under argon atmosphere. The samples were characterized by a scanning electron microscope (SEM) (Philips XL 30) equipped with an energy dispersive X-ray (EDAX) microanalysis with gold coating. Crystallographic measurements of compound 1 were carried out at 295 K using a Bruker APEX-II CCD area-detector diffractometer. The intensity data were collected using graphite monochromated Mo-K$_\alpha$ radiation (λ= 0.71073 Å).

Absorption corrections were applied with the program SADABS [36]. The structure was solved by direct methods SHELXS-97 [37], and refined by full-matrix least-squares techniques on F^2 using SHELXL-97 [37] with refinement of F^2 against all reflections. All non-hydrogen atoms were refined anistropically and hydrogen atoms were located and included in their calculated positions. The final full-matrix, least-squares refinement on F^2 was applied for all observed reflections [I> 2σ(I)]. Crystallographic data and details of data collections and structure refinements of compound 1 are listed in Table 1.

2.2. Synthesis of [Cd(dmph)I₂] (1) as single crystal

To isolate single crystals of [Cd(dmph)I$_2$] (1), 2,9-dimethyl-1,10-phenanthroline (0.5 mmol, 0.104 g), cadmium(II) acetate (0.5 mmol, 0.133 g) and potassium iodide (1 mmol, 0.166 g) were placed in the main arm of a branched tube. Methanol was carefully added to fill both arms. The tube was sealed and the ligand-containing arm immersed in an oil bath at 60 $^\circ$C while the other arm was kept at ambient temperature. After 4 days, colorless crystals that deposited in the cooler arm were isolated, filtered off, washed with water and air dried (0.311 g, yield: 77%), decomposition point ~ 260 $^\circ$C. Anal. Calcd. for C$_{14}$H$_{12}$N$_2$CdI$_2$ (%): C, 29.27; H, 2.10; N, 4.88. Found (%): C, 29.19; H, 2.13; N, 4.79. FT-IR (cm^{-1}) selected bands: 3424(b), 3048(w), 1616(w), 1590(w), 1502(s), 1435(w), 1366(w), 1149(w), 1024(w), 864(s), 774(w), 728(w), 655(w), 548(w) and 432(w).

2.3. Synthesis of nano-structured [Cd(dmph)I₂] (1) by the sonochemical method

In order to prepare compound 1 at nano-scale, 15 ml methanolic solution of cadmium(II) acetate (1.5

Table 1. Crystal data and structure refinement for compound **1**.

Empirical formula	C$_{14}$H$_{12}$N$_2$I$_2$Cd
Formula weight	574.47
Temperature (K)	295
Wavelength (Å)	0.71073
Crystal system	Monoclinic
Space group	*C2/c*
Unit cell dimensions	
a(Å)	15.714(3)
b (Å)	11.617(2)

c (Å)	9.884(2)
α (°)	90
β (°)	114.65(3)
γ (°)	90
Volume (Å^3)	1639.9(7)
Z	4
Density (calculated) (g/cm^3)	2.327
Absorption coefficient (mm^{-1})	5.085
F(000)	1056
Crystal size (mm^3)	0.09×0.15×0.24
Theta range for data collection (°)	2.3-26
Index ranges	$-19 \leq h \leq 19$;
	$-14 \leq k \leq 12$;
	$-9 \leq l \leq 12$
Reflections collected	4010
Independent reflections (R_{int})	1546 [$R_{int} = 0.091$]
Absorption correction	Numerical
Refinement method	Full-matrix
	Least-squares on F^2
Data/restraints/parameters	1356/0/89
Goodness-of-fit (GOF) on F^2	1.07
Final R indices [I > 2σ (I)]	$R_1 = 0.0429$
	$wR_2 = 0.0929$
R Indices (all data)	$R_1 = 0.0521$
	$wR_2 = 0.0976$
Largest difference in peak and hole (e.Å^{-3})	1.10 and -1.13

$R_1 = \sum ||F_o| - |F_c|| / \sum |F_o|$, $wR_2 = [\sum (w(F_o^2 - F_c^2)^2) / \sum w(F_o^2)^2]^{1/2}$

mmol, 0.399 g) and KI (3 mmol, 0.498 g) in a vessel was positioned in a high-density ultrasonic probe, operating at 20 kHz with a maximum power output of 600 W. Into this solution 5 ml methanolic solution of the neocuproine ligand (1.5 mmol, 0.312 g) was added dropwise. The precipitates were isolated by centrifugation (4000 rpm, 15 min), washed with water and acetone to remove residual impurities and finally dried in air (0.892 g, yield: 74%), decomposition point ~ 250 °C. Elemental analysis found (%): C, 29.28; H, 2.09; N, 4.84. FT-IR (cm^{-1}) selected bands observed were: 3434(b), 3048(w), 1618(w), 1590(w), 1502(s), 1436(w), 1367(w), 1150(w), 1024(w), 864(s), 773(w), 728(w), 654(w), 550(w) and 429(w).

2.4. Synthesis of CdO and CdI$_2$ nanoparticles by thermal decomposition of compound 1

For the preparation of cadmium(II) oxide nanoparticles, calcination of the compound 1 was performed at 700 °C with heating rate 5 °C/min under air atmosphere. The powder XRD diffraction shows that calcination was completed and the entire organic compound was

decomposed. The XRD pattern shows the product is CdO. Cadmium(II) iodide nanoparticles were prepared by degradation of the compound 1 by the hydrothermal method. In this procedure, 0.6 g compound 1 was dissolved in 20 ml water. The solution was charged into a 50 ml Teflon-lined stainless steel autoclave and heated at 150 °C for 48 h. After the autoclave was cooled to room temperature, the product was filtered, dried and characterized.

3. Results and discussion

Reaction between neocuproine with a mixture of cadmium(II) acetate and potassium iodide under ultrasonic irradiation leads to the formation of a Cd(II) nano coordination compound, [Cd(dmph)I$_2$] (1). Single crystals of compound 1, suitable for X-ray crystallography, were prepared by a heat gradient applied to a methanolic solution of the reagents (the ''branched tube method'') [38]. The structures were confirmed by FT-IR, elemental analysis and powder X-ray diffraction (XRD) patterns. Scheme 1 summarizes the synthesis methods.
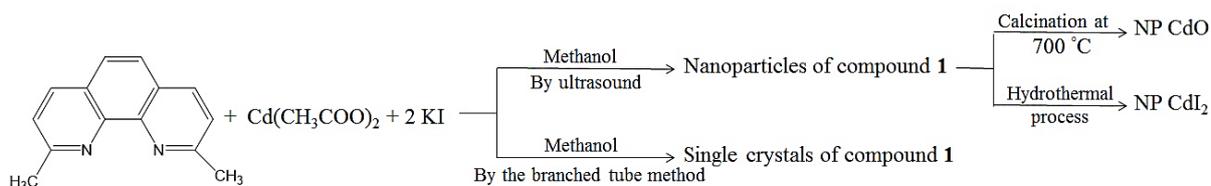
Scheme 1. Materials produced and synthetic methods.

The compound displayed distinct melting point and elemental analysis consistent with the formula $C_{14}H_{12}N_2CdI_2$. Elemental analysis and FT-IR spectra of the complex as nano and single crystalline data indicate acceptable matches for the structure, indicating that products obtained by the branched-tube method and ultrasonic irradiation are identical.

The FT-IR spectra of the nanoparticles and of the single crystalline material in the frequency range from 400-

3500 cm^{-1} are indistinguishable (Fig. 1) and show the same characteristic absorption bands for the neocuproine ligand [30]. The only differences among these characteristic peaks were the band intensities or a slight shift in the band positions. All distinct bands of neocuproine are illustrated in Table 2, and assigned to corresponding vibration [39].
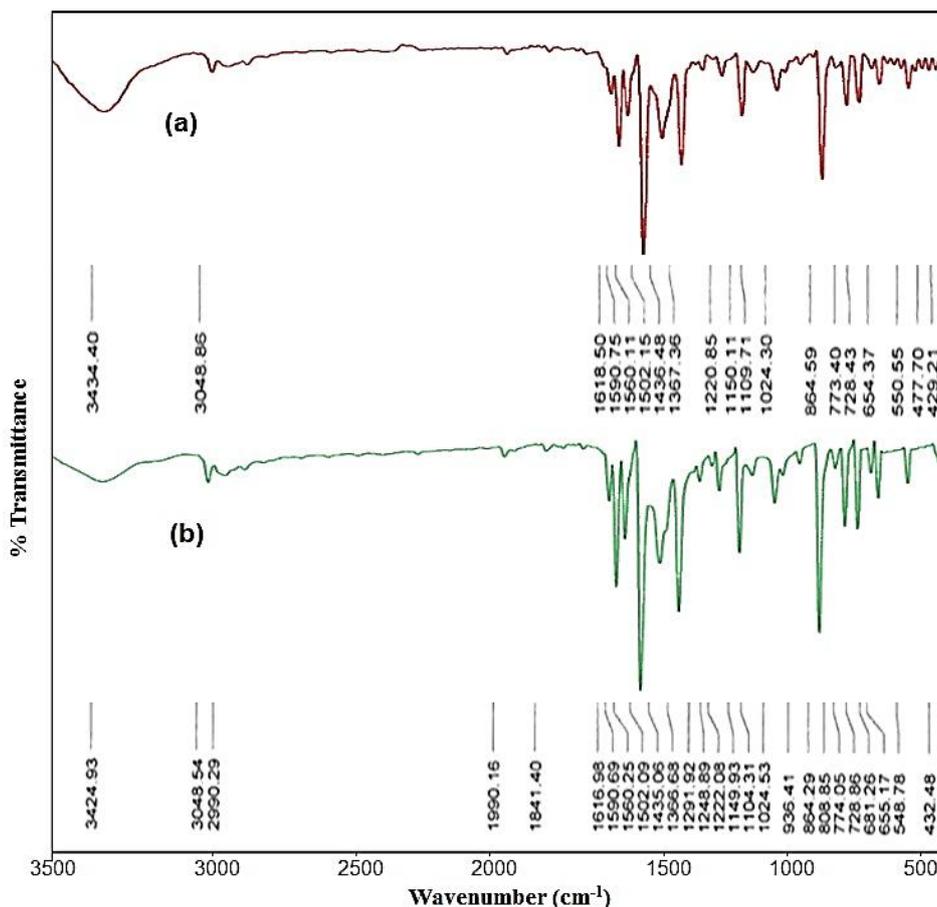

Fig. 1. FT-IR spectra of (a) nanoparticles of compound **1** prepared by sonochemical method, and (b) bulk materials as synthesized of **1**.

Table 2. FT-IR absorption peaks of the neocuproine [38].

Peak (cm^{-1})	Assignments
3447 (w)	Free υ (N–H)
3064, 3036	Aromatic υ (C–H)
2990–2920	υ CH$_3$
1671 (m), 1614 (m), 1591 (m), 1550 (w), 1508 (m), 1494(vm), 1423 (w)	υ (C=C), υ (C=N)
850, 732	out-of-plane CH in center ring

The structure of compound 1 was characterized by the single-crystal X-ray diffraction technique (Table 1).

The molecular structure of the fundamental building unit for 1 is shown in Fig. 2.
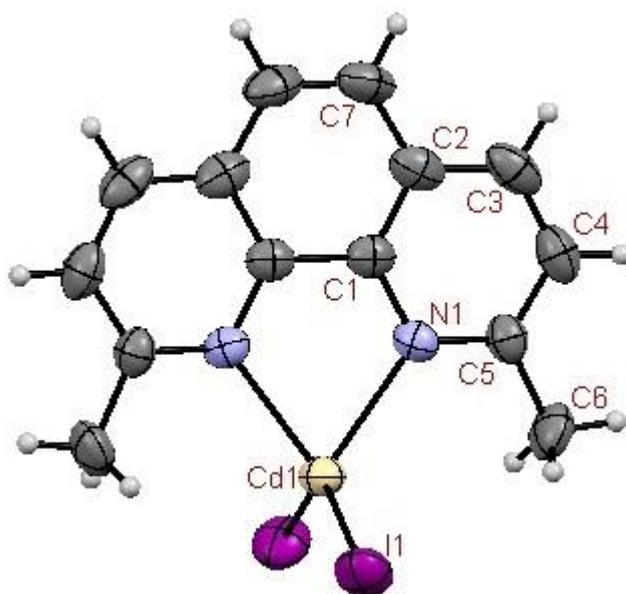
Fig. 2. Molecular structure and coordination environment of the compound [Cd(dmph)I$_2$] (**1**).

The Cd(II) ion is four-coordinated in a distorted tetrahedral configuration with two N atoms from a neocuproine ligand and two terminal I atoms. The corresponding bond lengths (Å) and angles (º) around the Cd(II) center are listed in Table 3.

Table 3. Selected bond lengths (Å) and angles (º) for compound **1**.

Cd1—I1	2.699(8)	I1—Cd1—N1	112.10(12)
Cd1—N1	2.308(5)	I1—Cd1—I1$_a$	129.75(4)
Cd1—N1$_a$	2.308(5)	I1—Cd1—N1$_a$	107.77(12)
N1—C1	1.373(7)	I1$_a$—Cd1—N1	107.77(12)
N1—C5	1.337(7)	N1—Cd1—N1$_a$	73.31(18)
C1-C2	1.393(9)	I1$_a$—Cd1—N1$_a$	112.10(12)
C1-C1$_a$	1.460(7)		

The packing of compound 1 is shown in Fig. 3. It is seen in Fig. 3, the neocuproine act as bi-dentate ligand to join the cadmium(II) centers via two nitrogen atoms from phenantroline rings and forms a 3D neutral framework. The title complex crystallizes in the monoclinic space group *C2/c* with four molecules per unit cell.

Fig. 4 shows the simulated XRD pattern from single crystal X-ray data of compound 1 (Fig. 4a) in comparison with the XRD pattern of the typical sample of compound 1 prepared by the sonochemical method (Fig. 4b). Acceptable matches, with slight differences in *2θ*, were observed between the simulated and experimental powder X-ray diffraction patterns.
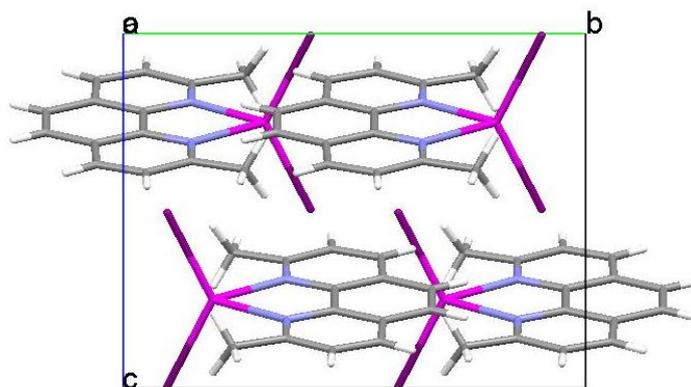
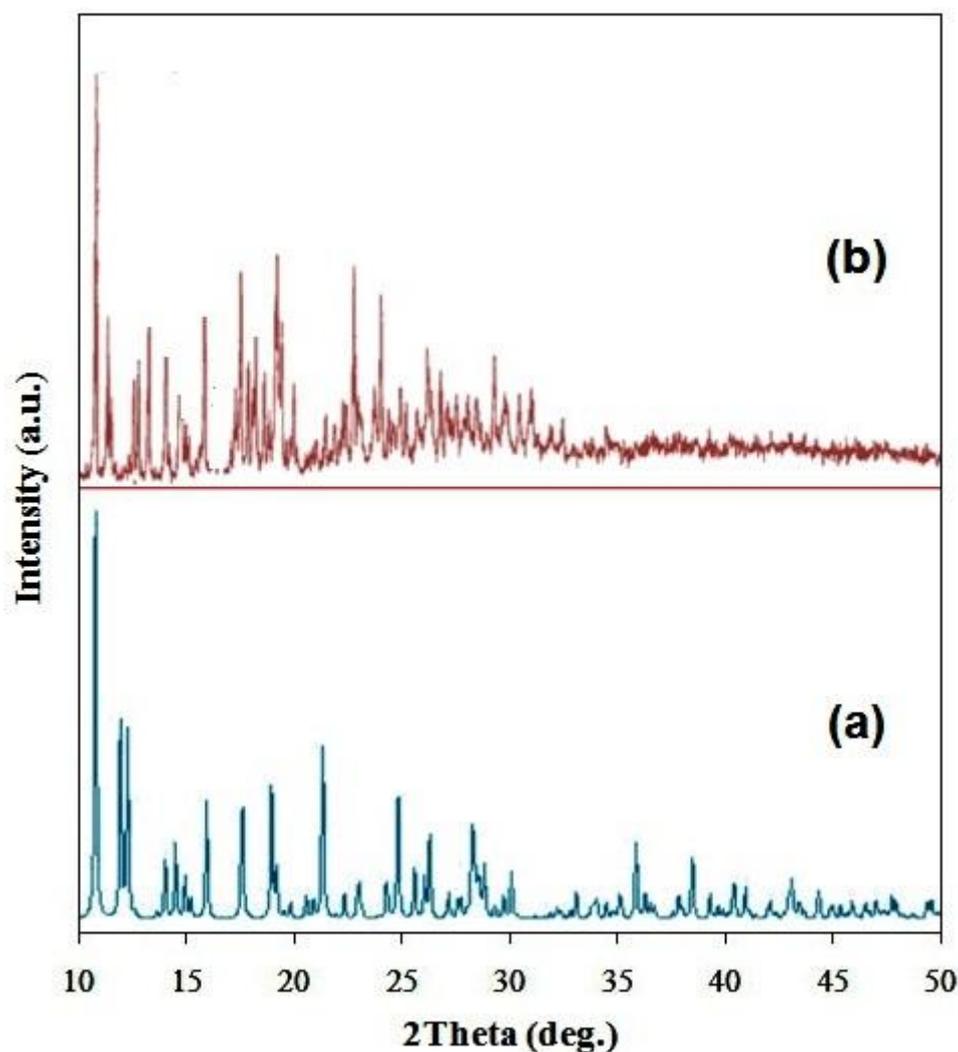

Fig. 3. The unit cell and packing of compound 1.

Fig. 4. XRD patterns; (a) simulated pattern based on single crystal data of compound 1, and (b) nanoparticles of compound 1 prepared by sonochemical method.

This indicates that the compound obtained by the sonochemical method as nanoparticles is identical to that obtained by single crystal diffraction. The significant broadening of the peaks indicates that the particles are of nanometer dimensions. The partical size estimated from the Scherrer formula is 96 nm. This calculation of particle size was obtained from values of the broadening of the XRD peaks ($D= 0.891\lambda/\beta cos\theta$, where D is the average grain size, λ is the X-ray wavelength (1.5418 Å), and θ and β are the diffraction angle and full-width at half maximum of an observed peak, respectively [40]) This value was in agreement with the value obtained from the SEM images (Fig. 5). The morphology and size of compound 1 prepared by the sonochemical method was characterized by scanning electron microscopy and is shown in Fig. 5. The SEM images shows that the morphology of the compound 1 comprises of spherically shaped particles with a broad distribution with particle sizes of about 90 nm.
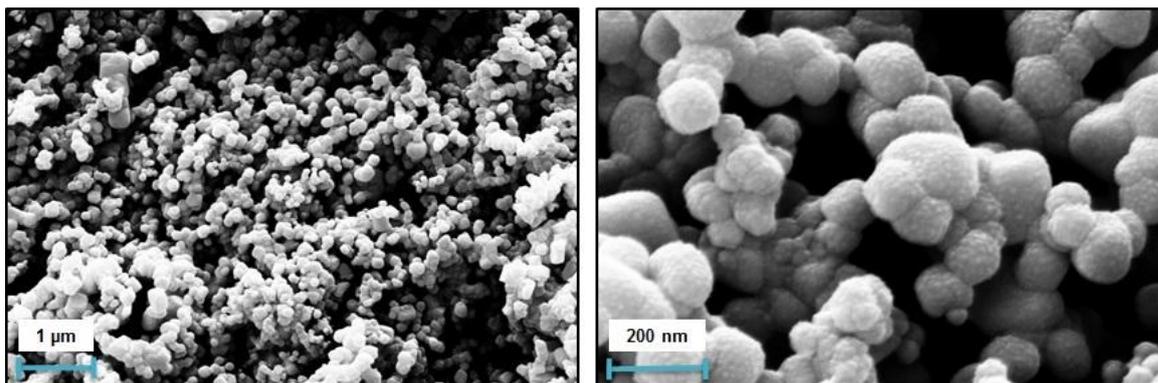
Fig. 5. SEM images of compound 1 nanoparticles prepared by sonochemical method in two different scale bars.

To examine the thermal stability of the nanoparticles and the single crystals of compound $[Cd(dmph)I_2]$ (1), thermal gravimetric (TG) and differential thermal analyses (DTA) were carried out between 25 and 600 °C under argon flow (Fig. 6).
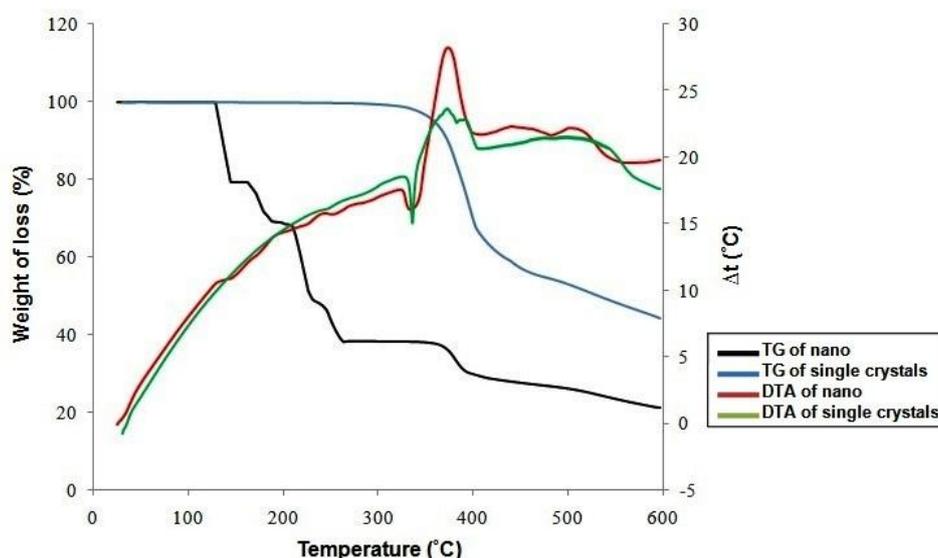

Fig. 6. Thermal behavior of compound 1 as bulk and nanoparticle.

The compound 1 as a bulk phase is very stable to temperature of 335 °C, at which temperature decomposition starts. Between 335 and 475 °C removal of dmph occurs with a mass loss of 35.40% (theoretically calculated as 36.25%). At higher temperatures, the residue, presumably CdI_2, was decomposed and mass loss calculations show that the final decomposition product is CdO. Compared to the bulky material, nanoparticles of compound 1 are much less stable and start to decompose at 130 °C. The TG curve exhibits five distinct decomposition stages between 130 and 390 °C with a total mass loss of 77.40% (theoretically calculated as 80.43%). Detectable decomposition of the nanoparticles of 1 thus begins at about 205 °C much earlier than that of its bulk counterparts, decomposition of iodine atoms taken place in two steps between 130 to 205 °C. This is probably due to the much higher surface to volume ratio of the nanoparticles, as more heat is needed to break the lattices of the bulk materials. Mass loss calculations of the end residue and the XRD pattern of the final

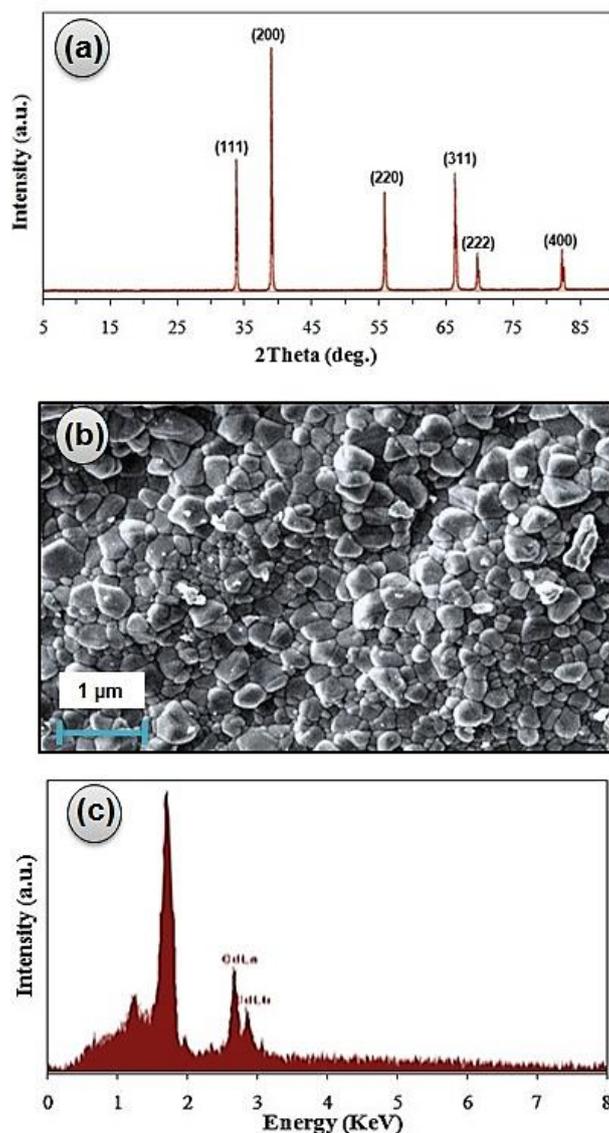decomposition product show the formation of CdO (Fig. 7a).

Fig. 7. (a) XRD pattern, (b) SEM photograph, and (c) EDAX analysis of CdO nanoparticles prepared by calcination of compound 1 at 700 °C.

Moreover, the DTA curves displays an endothermic peak at 335 °C and an exothermic peaks at 370 °C for the single crystals of compound 1 (Fig. 6). The DTA curve of the nano-structured material has the same appearance as those of their single crystalline counterparts and the endo- and exothermic effects are retained for nano-structured 1. Some differences between the maximum intensities indicate, in agreement with TGA results, a somewhat lower stability of the nano-structures when compared with their bulk materials.

Fig. 7a provides the XRD pattern of the residue obtained from thermal decomposition of compound 1, that were prepared from sonochemical method, at 700 °C with a heating rate of 5 °C min^{-1} under air atmosphere. The obtained pattern matches with the standard pattern of Monteponite cadmium(II) oxide with the lattice parameters (a= 4.6953 Å, S.G.= Fm3m and Z= 4) which is the same as the reported values (JCPDS card number 05-0640). No characteristic peaks of impurities are detected. The broadening of the peaks indicated that the particles were at the nanometer scale,

which is in agreement with that observed from SEM image (Fig. 7b). Average size of the particles was estimated from Scherrer formula, average sizes of the particles are 65 nm for CdO nanoparticles. The morphology and size of the cadmium(II) oxide nanoparticles were studied by SEM (Fig. 7b), which shows uniform nanometer scale quasi-spherical CdO nanoparticles. The particles have a good size distribution. Furthermore, EDAX was performed on the CdO nanoparticles (Fig. 7c). The EDAX spectrum shows the presence of cadmium as the only elementary component. This indicates that the product from direct calcination of compound 1 is pure CdO nanoparticles. Cadmium(II) iodide nanoparticles were prepared by degradation of the compound 1 by the hydrothermal

method is shown in Fig. 8a and indicates a relatively low homogeneity. The EDAX spectrum (Fig. 8b) shows the presence of cadmium and iodine as the only elementary components. We thus report the preparation of CdO and CdI_2 nanoparticles from Cd(II) supramolecular compound, $[Cd(dmph)I_2]$ (1), as a nontoxic new precursor by thermal decomposition method. Among various techniques for synthesis of transition metal oxide nanoparticles, thermal decomposition is more favorable, because we can control process conditions, particle size, particle crystal structure and purity. Moreover, it has the advantages of short time, high yield, low cost and low power consumption.
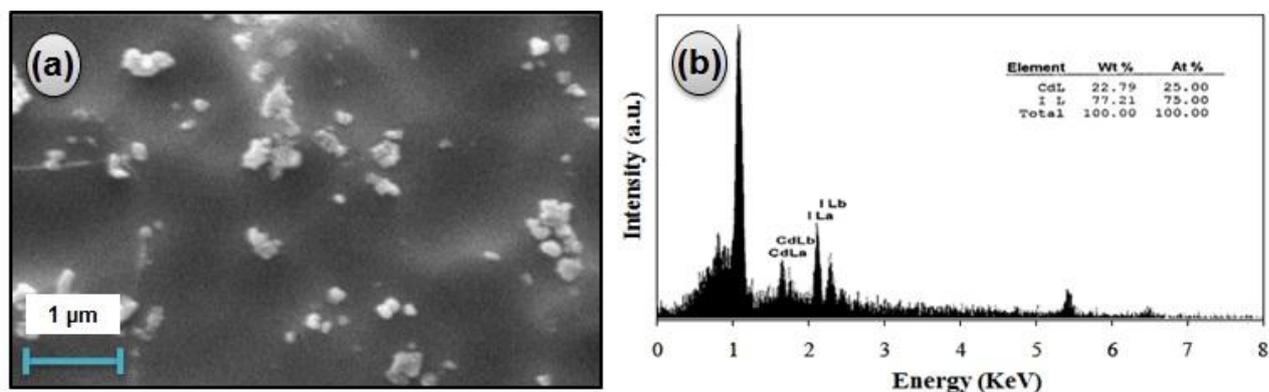

Element	Wt %	At %
Cd L	22.79	25.00
I L	77.21	75.00
Total	100.00	100.00

Fig. 8. (a) SEM photograph, and (b) EDAX analysis of CdI_2 nanoparticles prepared by hydrothermal process of compound 1.

4. Conclusion

A cadmium(II) coordination compound, $[Cd(dmph)I_2]$ (1), was synthesized using a thermal gradient under sonochemical irradiation. Compound 1 manifests as nano-sized particles. The crystal structure of compound 1 was determined by single-crystal X-ray diffraction and reveals that Cd(II) ion is four-coordinated in a distorted tetrahedral configuration with two N atoms from neocuproine ligand and two terminal iodine atoms. TG studies indicate that a decrease in the particles size of compound 1 to a few dozen nanometers results in lower thermal stability when compared to the single crystalline samples. Hydrothermal decomposition and calcination of compound 1 under air atmosphere lead to different types of nano-structured

materials. The nano-sized Cd(II) complex is a suitable non-toxic precursor for preparation of nano-scale CdO and CdI_2 materials with interesting morphologies. This method of preparation has presumably some advantages such as shorter reaction timesand better yields to produce nano-sized particles of the complex.

5. Supplementary Material

Crystallographic data for the structure reported in this article has been deposited with the Cambridge Crystallographic Data Centre as supplementary publication no. CCDC-782507. Copies of the data can be obtained on application to CCDC, 12 Union Road, Cambridge CB2 1EZ, UK [Fax: +44-1223/336033; E-mail: deposit@ccdc.cam.ac.uk].

References

[1] H.H. Nalwa, Boston: Academic Press, (2000).

[2] M. Ranjbar, M. Yousefi, R. Nozari, S. Sheshmani, *Int. J. Nanosci. Nanotechnol.,* **9** (2013) 203.

[3] M. Ranjbar, M. Yousefi, M. Lahooti, A. Malekzadeh, *Int. J. Nanosci. Nanotechnol.,* **8** (2012) 191.

[4] K.-T. Wong, J.-M. Lehn, S.-M. Peng, G.-H. Lee, *Chem. Commun.,* (2000) 2259.

[5] A.G. Bunn, P.J. Carroll, B.B. Wayland, *Inorg. Chem.,* **31** (1992) 1297.

[6] M.A.M. Abu-Youssef, A. Escuer, D. Gatteschi, M.A.S. Goher, F.A. Mautner, R. Vicente, *Inorg. Chem.,* **38** (1999) 5716.

[7] A. Tanatani, M.J. Moi, J.S. Moore, *J. Am. Chem. Soc.,* **123** (2001) 1792.

[8] M. Fujita, Y.J. Kwon, S. Washizu, K.J. Ogura, *J. Am. Chem. Soc.,* **116** (1994) 1151.

[9] B. Notash, N. Safari, A. Abedi, V. Amani, H.R. Khavasi, *J. Coord. Chem.,* **62** (2009) 1638.

[10] Z. Rashidi Ranjbar, A. Morsali, *Polyhedron,* **30** (2011) 929.

[11] G.H. Shahverdizadeh, A. Morsali, *J. Inorg. Organomet. Polym.,* **21** (2011) 694.

[12] M. Payehghadr, V. Safarifard, M. Ramazani, A. Morsali, *J. Inorg. Organomet. Polym.,* **22** (2012) 543.

[13] D.M. Ciurtin, Y.-B. Dong, M.D. Smith, T. Barclay, H.-C. Loye, *Inorg. Chem.,* **40** (2001) 2825.

[14] M.-H. Kim, Y.-U. Kwon, *J. Phys. Chem. C,* **113** (2009) 17176.

[15] M. Burbano, D.O. Scanlon, G.W. Watson, *J. Am. Chem. Soc.,* **133** (2011) 15065.

[16] D.M. Yufanyi, J.F. Tendo, A.M. Ondoh, J.K. Mbadcam, *J. Mat. Sci. Res.,* **3** (2014) 1.

[17] A.S. Aldwayyan, F.M. Al-Jekhedab, M. Al-Noaimi, B. Hammouti, T.B. Hadda, M. Suleiman, I. Warad, *Int. J. Electrochem. Sci.,* **8** (2013) 10506.

[18] V. Safarifard, A. Morsali, *Ultrason. Sonochem.,* **19** (2012) 1227.

[19] M. Ghosh, C.N.R. Rao, *Chem. Phys. Lett.,* **393** (2004) 493.

[20] W. Dong, C. Zhu, *Opt. Mater.,* **22** (2003) 227.

[21] M. Ranjbar, E. Malakooti, S. Sheshmani, *J. Chem.,* (2013) doi: 10.1155/2013/560983.

[22] N. Akbarzadeh Torbati, A.R. Rezvani, N. Safari, V. Amani, H.R. Khavasi, *Acta Cryst. E,* **66** (2010) m1236.

[23] A. Dehghani, M.M. Amini, E. Najafi, A. Tadjarodi, B. Notash, *Acta Cryst. E,* **68** (2012) m811.

[24] B. S. Wang, H. Zhong, *Acta Cryst. E,* **65** (2009) m1156.

[25] J.H. Bang, K.S. Suslick, *Adv. Mater.,* **22** (2010) 1039.

[26] W.-J. Son, J. Kim, J. Kim, W.-S. Ahn, *Chem. Commun.,* (2008) 6336.

[27] L.-G. Qiu, Z.-Q. Li, Y. Wu, W. Wang, T. Xu, X. Jiang, *Chem. Commun.,* (2008) 3642.

[28] M. Yousefi, M. Ranjbar, *J. Inorg. Organomet. Polym.,* **27** (2017) 633.

[29] M. Ranjbar, M. Yousefi, *J. Inorg. Organomet. Polym.,* **24** (2014) 652.

[30] M. Ranjbar, M. Lahooti, M. Yousefi, A. Malekzadeh, *J. Iran. Chem. Soc.,* **11** (2014) 1257.

[31] M. Ranjbar, M. Nabitabar, Ö. Çelik, M. Yousefi, *J. Iran. Chem. Soc.,* **12** (2015) 551.

[32] M. Ranjbar, M. Yousefi, *Iran. J. Sci. Technol. Trans. Sci.,* (2016) doi: 10.1007/s40995-016-0069-9.

[33] M. Ranjbar, M. Yousefi, *Int. J. Nanosci. Nanotechnol.,* **12** (2016) 109.

[34] M. Rafigh Esmaeel Zaee, H. Saravani, M. Shahraki, *Journal of Applied Chemistry*, **13** (2018) 83.

[35] Mercury 1.4.1, Copyright Cambridge Crystallographic Data Centre, 12 Union Road, Cambridge, CB2 1EZ, UK, 2001–2005.

[36] Bruker, SADABS. Bruker AXS Inc., Madison, Wisconsin, USA, (2007).

[37] G.M. Sheldrick, *Acta Cryst. A,* **64** (2008) 112.

[38] A. Morsali, M.Y. Masoomi, *Coord. Chem. Rev.,* **253** (2009) 1882.

[39] V. Viossat, P. Lemoine, E. Dayan, N.-H. Dung, B. Viossat, *J. Mol. Struc.,* **741** (2005) 45.

[40] H. P. Klug, L. E. Alexander, New York: Wiley, (1974).